Sleeping Beauty mutagenesis reveals cooperating mutations and pathways in pancreatic adenocarcinoma

Karen M. Mann[a,1], Jerrold M. Ward[a], Christopher Chin Kuan Yew[a], Anne Kovochich[b], David W. Dawson[b], Michael A. Black[c], Benjamin T. Brett[d], Todd E. Sheetz[d,e,f], Adam J. Dupuy[g], Australian Pancreatic Cancer Genome Initiative[h,2], David K. Chang[i,j,k], Andrew V. Biankin[i,j,k], Nicola Waddell[l], Karin S. Kassahn[l], Sean M. Grimmond[l], Alistair G. Rust[m], David J. Adams[m], Nancy A. Jenkins[a,1], and Neal G. Copeland[a,1,3]

[a]Division of Genetics and Genomics, Institute of Molecular and Cell Biology, Singapore 138673; [b]Department of Pathology and Laboratory Medicine and Jonsson Comprehensive Cancer Center, David Geffen School of Medicine at University of California, Los Angeles, CA 90095; [c]Department of Biochemistry, University of Otago, Dunedin, 9016, New Zealand; [d]Center for Bioinformatics and Computational Biology, University of Iowa, Iowa City, IA 52242; [e]Department of Biomedical Engineering, University of Iowa, Iowa City, IA 52242; [f]Department of Ophthalmology and Visual Sciences, Carver College of Medicine, University of Iowa, Iowa City, IA 52242; [g]Department of Anatomy and Cell Biology, Carver College of Medicine, University of Iowa, Iowa City, IA 52242; [h]Australian Pancreatic Cancer Genome Initiative; [i]Cancer Research Program, Garvan Institute of Medical Research, Darlinghurst, Sydney, New South Wales 2010, Australia; [j]Department of Surgery, Bankstown Hospital, Bankstown, Sydney, New South Wales 2200, Australia; [k]South Western Sydney Clinical School, Faculty of Medicine, University of New South Wales, Liverpool, New South Wales 2170, Australia; [l]Queensland Centre for Medical Genomics, Institute for Molecular Bioscience, University of Queensland, Brisbane, Queensland 4072, Australia; and [m]Experimental Cancer Genetics, Wellcome Trust Sanger Institute, Hinxton, Cambridge CB10 1HH, United Kingdom

Pancreatic cancer is one of the most deadly cancers affecting the Western world. Because the disease is highly metastatic and difficult to diagnosis until late stages, the 5-y survival rate is around 5%. The identification of molecular cancer drivers is critical for furthering our understanding of the disease and development of improved diagnostic tools and therapeutics. We have conducted a mutagenic screen using *Sleeping Beauty* (*SB*) in mice to identify new candidate cancer genes in pancreatic cancer. By combining *SB* with an oncogenic *Kras* allele, we observed highly metastatic pancreatic adenocarcinomas. Using two independent statistical methods to identify loci commonly mutated by *SB* in these tumors, we identified 681 loci that comprise 543 candidate cancer genes (CCGs); 75 of these CCGs, including *Mll3* and *Ptk2*, have known mutations in human pancreatic cancer. We identified point mutations in human pancreatic patient samples for another 11 CCGs, including *Acvr2a* and *Map2k4*. Importantly, 10% of the CCGs are involved in chromatin remodeling, including *Arid4b*, *Kdm6a*, and *Nsd3*, and all *SB* tumors have at least one mutated gene involved in this process; 20 CCGs, including *Ctnnd1*, *Fbxo11*, and *Vgll4*, are also significantly associated with poor patient survival. *SB* mutagenesis provides a rich resource of mutations in potential cancer drivers for cross-comparative analyses with ongoing sequencing efforts in human pancreatic adenocarcinoma.

Pancreatic ductal adenocarcinoma is one of the most deadly forms of cancer. In the United States, the rate of mortality is nearly equal to the rate of new diagnoses (1). Early disease detection is rare, and of those patients diagnosed with early-stage disease, only 20% are candidates for surgical resection. Approximately 50% of patients develop highly metastatic disease, for which current treatment regimens provide little increase in longevity (2). Clearly, there is a need for better biomarkers of disease and the identification of new therapeutic targets, particularly for metastatic disease.

Human pancreatic cancer develops from preinvasive neoplasias, typically intraepithelial neoplasias (PanINs), although intraductal papillary mucinous neoplasia and mucinous cystic neoplasia can also give rise to adenocarcinoma (3). The majority of pancreatic adenocarcinoma is of ductal origin and contains a large desmoplastic component thought to promote tumorigenesis by modulating the tumor microenvironment. Oncogenic *KRAS* mutations are found in 90% of human tumors, and they appear in early PanIN (4). The accumulation of additional inactivating driver mutations in *P16/CDKN2A*, *TP53*, and *SMAD4* occurs with high frequency in later-stage PanIN, and these mutations are likely required for tumor progression to invasive adenocarcinoma.

Recent high-throughput sequencing efforts have shown that the majority of somatic point mutations in primary pancreatic adenocarcinoma are missense mutations and that most occur at low frequency (5). Pancreatic cancers exhibit a very unstable genome, and through whole-genome sequencing efforts, a specific type of genomic instability, termed fold-back inversion, has been elucidated (6). It is clear from these data that characterization of a large number of tumors is required to fully capture the molecular heterogeneity of the disease and identify the specific mutations and signaling pathways that drive disease progression.

Pancreatic cancer has been successfully modeled in the mouse by driving expression of oncogenic *Kras* in the pancreas either alone or combined with inactivating alleles of homologs of known human pancreatic cancer drivers (7–11), including *Smad4* and *Trp53*. All of these models show progressive neoplastic lesions, termed mPanIN (12), and develop locally invasive, and in some cases, metastatic ductal adenocarcinoma. Although these models have furthered our understanding of pancreatic cancer biology, new mutations that drive cancer development have not been uncovered in these efforts.

We have taken an independent approach to identify genes commonly mutated in a mouse model of pancreatic cancer. We performed an insertional mutagenesis screen using the inducible *Sleeping Beauty* (*SB*) transposon system (13) in combination with an oncogenic *Kras* pancreatic cancer model. This approach is a powerful means to identify mutations that cooperate with oncogenic *Kras* to drive tumorigenesis in the mouse, because each mutation is mapped using a transposon tag. Mice with *SB* insertional mutagenesis exhibit all stages of mPanIN lesions. *SB* decreases the latency of pancreatic tumorigenesis compared with oncogenic *Kras* alone and increases both the severity and

multiplicity of ductal adenocarcinomas. Multiple metastases are also observed in a subset of animals.

Using the transposon tag, we identify 543 candidate cancer genes (CCGs) that show significant enrichment for transposon insertions in *SB*-driven pancreatic cancer. Several signaling pathways and cellular processes are enriched in these CCGs, most significantly TGF-β signaling and chromatin modification. We find 20 genes not previously associated with pancreatic cancer that are significantly associated with poor patient outcome. We also identified point mutations in human homologs of 11 *SB* CCGs by exome sequencing of patient samples. *SB* mutagenesis is an important tool for the discovery of potential molecular drivers in pancreatic cancer and complements current human sequencing efforts by providing an enriched dataset for cooperating mutations involved in pancreatic adenocarcinoma.

Results

SB Drives Pancreatic Tumorigenesis in the Mouse. To identify genes that cooperate with activated *Kras* in pancreatic tumorigenesis, we performed a forward genetic screen in mice carrying a conditional oncogenic $Kras^{G12D}$ allele (LSL-$Kras^{G12D}$) (14) using *SB* transposon-mediated insertional mutagenesis (13). Mice carrying the LSL-$Kras^{G12D}$ allele were crossed to mice carrying a pancreatic-specific *Pdx1-Cre* driver (15) to remove the floxed stop cassette (LSL) and activate expression of oncogenic $Kras^{G12D}$ in the pancreas. These mice were then crossed to a compound transgenic line containing up to 350 copies of a mutagenic *SB* transposon from a single donor site in the genome, and an inducible *SB* floxed stop transposase allele knocked into the ubiquitously expressed *Rosa26* locus (*Rosa26-LSL-SB11*) (13). Because of the presence of the floxed stop cassette, the transposase is not expressed unless Cre recombinase protein is present. We used two transposon transgenic lines, T2Onc2 and T2Onc3, located on different chromosomes to obtain insertion data from the entire genome. Typically, data from a transposon donor chromosome are disregarded because of computational limitations in discerning local hopping events from selected transposition events. T2Onc2 carries a strong promoter derived from the murine stem cell virus, whereas T2Onc3 carries the ubiquitously expressed CAG promoter to activate expression of proto-oncogenes. Both transposons also carry splice acceptor sites in both orientations and a bidirectional polyA signal and they can, therefore, inactivate the expression of tumor suppressor genes when integrated within the coding region in either orientation.
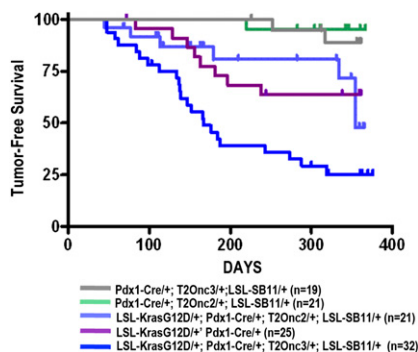

Fig. 1. *SB* mutagenesis drives pancreatic tumorigenesis in the mouse. Five cohorts of mice were aged and monitored for pancreatic tumor development. All five cohorts carried the *Pdx1-Cre* driver to activate oncogenic $Kras^{G12D}$ and *SB* transposase in the pancreas. $Kras^{G12D}$ was required for the high frequency induction of pancreatic tumors. Animals with oncogenic $Kras^{G12D}$ and T2Onc3 died significantly earlier than animals in the other four cohorts (*P* < 0.001). *n* is the number of animals aged for tumors.

Five different cohorts of mice carrying different combinations of alleles were bred and aged for tumor formation (Fig. 1). We observed a significant decrease in tumor-free survival when oncogenic $Kras^{G12D}$ was combined with T2Onc3 but not T2Onc2 (Fig. 1), although the tumors were more histologically advanced with both T2Onc2 and T2Onc3 mutagenesis compared with $Kras^{G12D}$ alone (Fig. 2). Gross inspection of the pancreas at necropsy revealed pancreatic masses that often involved neighboring organs (Fig. 2*A*). Metastatic nodules on the liver (Fig. 2*B*) and lymph nodes (Fig. 2*C*) were also often seen. The majority of the animals with oncogenic $Kras^{G12D}$ developed early mPanIN lesions as previously reported (8) (Fig. 2 *D* and *E*). Six animals with oncogenic $Kras^{G12D}$ alone also developed noninvasive early adenocarcinoma (Fig. S1 *A–C*), whereas two animals developed spontaneous adenocarcinoma; 19 animals from the $Kras^{G12D}$; T2Onc2 and $Kras^{G12D}$;T2Onc3 cohorts developed adenocarcinoma, whereas 14 of these animals developed highly invasive metastatic adenocarcinoma (Fig. 2*F*). Most of the $Kras^{G12D}$; T2Onc3 animals developed multiple primary pancreatic tumors (two to three on average), and all had metastases to multiple sites associated with the human disease, including lung (Fig. 2*G*) and lymph nodes (Fig. 2 *H* and *I*). Three animals from the *SB* cohorts lacking oncogenic $Kras^{G12D}$ also developed invasive adenocarcinoma.

Tumors from all cohorts were histologically characterized for markers commonly associated with ductal adenocarcinoma. Early mPanIN lesions showed high mucin content, which was shown by Alcian blue staining, that was reduced in late-stage mPanIN lesions and largely absent in adenocarcinomas (Fig. S1*D*). Mucin accumulates in human PanIN and may serve as an early biomarker of disease (16). Fibrosis was also observed in many of the adenocarcinomas, and these adenocarcinomas stained positive for both smooth muscle actin and Masson's Trichome for
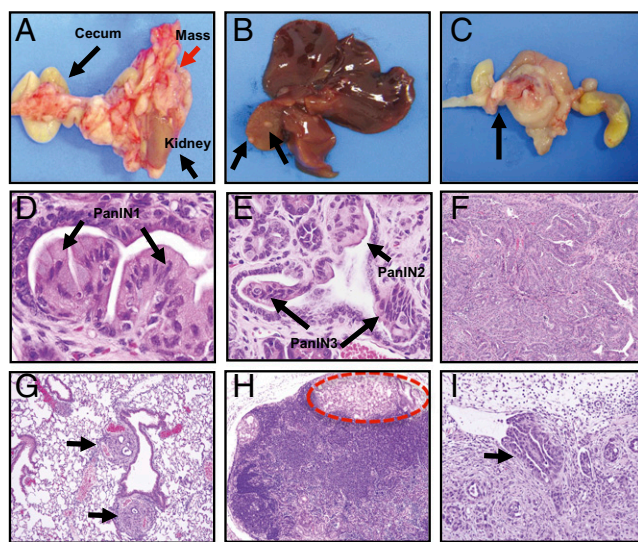

Fig. 2. Histopathological classification of pancreatic lesions. *SB* mutagenesis generated pancreatic lesions at all stages of tumor progression. (*A*) Mice exhibited pancreatic masses that often involved neighboring organs such as the kidney and cecum. Metastatic nodules on the liver (*B*) and lymph nodes (*C*) were also often visible on gross inspection. A spectrum of mPanIN lesions was also observed with oncogenic $Kras^{G12D}$, including early mPanIN1B lesions (*D*) showing enlarged cell volume and high mucin content in addition to mPanIN2 and mPanIN3 lesions (*E*). Nineteen animals from the T2Onc2 and T2Onc3 cohorts developed ductal pancreatic tumors. Fourteen animals developed multiple invasive ductal adenocarcinomas (*F*). Several animals also developed multiple metastatic lesions to the lung (*G*) and lymph nodes (*H* and *I*).

collagen (Fig. S1 *E* and *F*). The presence of fibrotic foci is a hallmark of pancreatic cancer, and high levels of smooth muscle actin were recently correlated with poor survival of patients with advanced pancreatic ductal adenocarcinomas (17). Pdx1 was also reexpressed in both adenocarcinomas and metastases (Fig. S1 *G–I*), and these lesions were of ductal origin, which was shown by cytokeratin-19 staining (Fig. S1 *J–L*).

Sequence Analysis of Transposon Insertion Sites Identifies Pancreatic CCGs. To identify genes that contribute to pancreatic tumor development in oncogenic $Kras^{G12D}$ mice, we PCR-amplified and sequenced the transposon insertion sites from 21 *SB*-induced pancreatic tumors isolated from 19 animals; 9 tumors were from T2Onc2 animals, and 12 tumors were from T2Onc3 animals (*Materials and Methods*). High-throughput sequencing using the Roche 454 Titanium platform identified 19,927 unique insertion sites that mapped to the mouse genome. These insertion sites were then analyzed using the Gaussian kernel convolution (GKC) method to identify common insertion sites (CISs) (*SI Materials and Methods*) (18). CISs are regions in the genome that contain more transposon insertions than expected by chance and are most likely to contain a pancreatic cancer gene. The GKC method used 30-, 50-, 75-, 120-, and 240-K kernel widths. The outputs for each convolution were merged, and insertions contained within the smallest kernel were used to define the CIS (Dataset S1). The merged GKC output identified 133 CISs after correcting for multiple testing ($P < 0.05$). The 133 CIS loci identified 136 CCGs

in addition to one Riken clone (*1700081L11Rik*), one genome marker (*D17Wsu92e*), and one predicted gene (*Gm1568*).

Mapping of the 19,927 unique *SB* insertions on a Circos plot (19), which visualizes genome data on a circular layout, showed that the transposon insertions were well-distributed across the genome, with about one-half of the insertions located in the plus strand (Fig. 3, orange lines) and one-half in the minus strand (Fig. 3, purple lines). The GKC CIS peaks (Fig. 3, black lines) were also fairly well-distributed across the mouse autosomes with the exception of chromosome 1, which was devoid of CISs (Fig. 3). This finding may reflect the fact that the T2Onc2 donor concatamer is located on chromosome 1, and all insertions on this chromosome in T2Onc2 tumors were disregarded in the statistical analysis for CISs because of the local hopping phenomenon.

The location and directionality of the transposon insertions can be used to predict whether each CCG may function as an oncogene or tumor suppressor (TS) gene. Transposon insertions tend to occur near the 5′ end of an oncogene in the same transcriptional orientation, where they promote gene expression from the strong promoter within the transposon. In contrast, insertions in TS genes tend to be distributed across the coding region with little orientation bias, consistent with gene inactivation. By mapping the orientation of the transposon with respect to the orientation of the mutated gene, the majority of pancreatic tumor CCGs are predicted to function as TS genes (Datasets S1 and S2). This finding is similar to what has been observed for CCGs identified in transposon screens performed in other types of solid tumors (20–22),
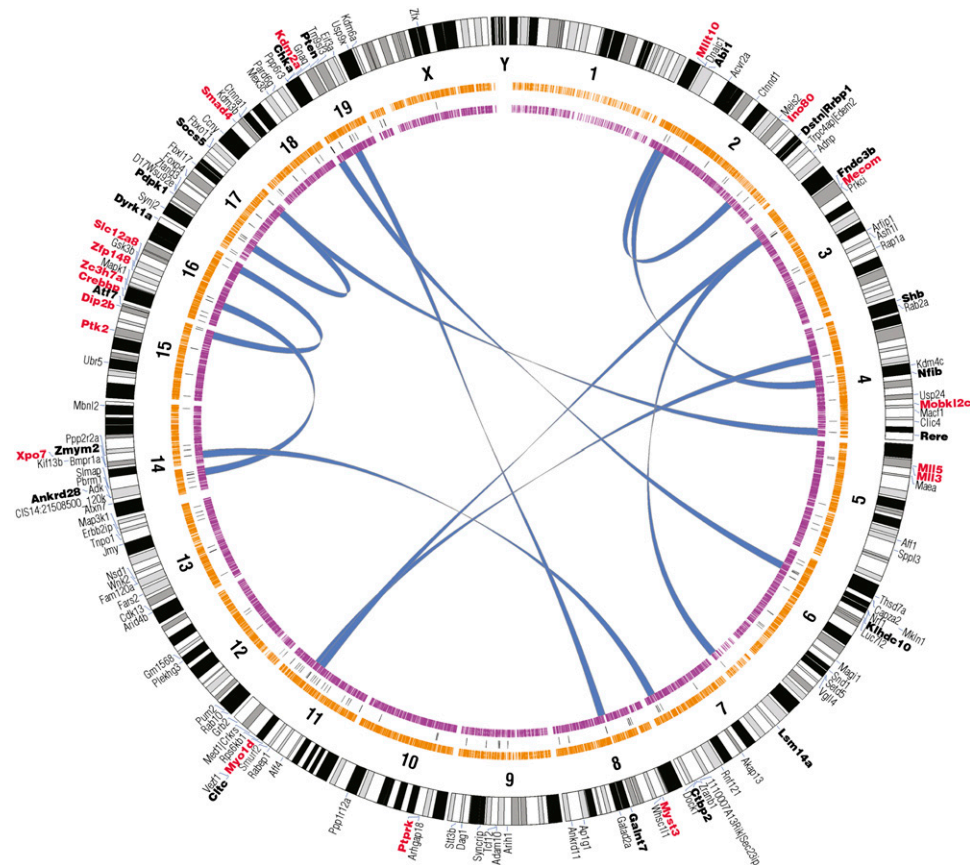

Fig. 3. Circos map of pancreatic cancer candidate cancer genes identified by the GKC method. Transposon insertions in the plus (orange lines) and minus (purple lines) strands show genome-wide coverage of mutagenesis. GKC CCGs are illustrated on the outer perimeter of the plot with their exact location denoted by a black line. Genes listed in red are mutated in human pancreatic cancer. The blue lines in the center connect bolded GKC CCGs that significantly co-occur in tumors (Fisher exact test, $P < 0.0003$).

but it is in contrast to what is observed in hematopoietic tumors, where the majority of CCGs seem to function as oncogenes (23).

Eighteen pancreatic GKC CCGs (14%) have also been previously shown to be mutated in human pancreatic cancer by exon resequencing or whole-genome sequencing (Dataset S2), and they are listed in red on the Circos plot in Fig. 3 (5, 6). These genes are involved in chromatin remodeling (*Crebbp*, *Ino80*, *Mecom*, *Mll5*, *Mll3*, *Kdm2a*, and *Myst3*), cell adhesion (*Ptk2* and *Ptprk*), protein transport (*Xpo7*), and transcriptional regulation (*Crebbp*, *Mllt10*, *Smad4*, and *Zfp148*). We also found significant enrichment for pancreatic GKC CCGs in regions containing genomic rearrangements in human pancreatic tumors (*n* = 6, *P* = 5.74E-03) (*Materials and Methods*) (6).

In addition, we found significant enrichment of GKC CCGs in the genes listed in the Cancer Gene Census (*n* = 19, *P* = 4.47E-11) (*Materials and Methods* and Dataset S2). The Cancer Gene Census is an ongoing effort to catalog those genes for which mutations have been causally implicated in cancer (24). Many CCGs are also mutated in other forms of human cancer, which was shown by exon resequencing or whole-genome sequencing, particularly in breast (23%) (25) and ovarian (50%) cancer (Dataset S2) (26). The degree of overlap with ovarian cancer is likely caused by the large sample size and sequence coverage of the recently annotated ovarian cancer genome by the Cancer Genome Atlas project (26).

Cooperating GKC CCGs in *SB*-Induced Pancreatic Tumors. To identify GKC CCGs that might cooperate in *SB*-induced pancreatic tumorigenesis, we performed pairwise comparisons using the Fisher exact test to look for significantly comutated loci in the pancreatic cancer genome. We identified 12 pairs of genes with *P* < 0.0003 from 862 pairwise comparisons (Dataset S3). These co-occurring relationships are shown in the Circos plot in Fig. 3 by the blue lines in the center connecting co-occurring GKC CCGs (bold font). More than one-half of these genes are involved in regulating cell growth and differentiation (*Atf7*, *Chka*, and *Pten*), apoptosis (*Rere*, *Ctbp2*, and *Shb*), or cell migration and invasion (*Abi1*, *Ankrd28*, *Dstn*, *Fndc3b*, *Galnt7*, *Pdpk1*, *Pten*, *Shb*, and *Socs5*).

GKC CCGs Are Enriched for Signaling Pathways and Processes Involved in Cancer. Similar to what has been reported for human tumors, pathway analysis of the pancreatic CCGs using Ingenuity Pathway Analysis (IPA) (27) suggests that the GKC CCGs function in a limited number of canonical signaling pathways, with many functioning in the same signaling pathway (Table 1) (5, 26, 28). Several of these pathways are important for human pancreatic cancer, including TGF-β, ERK/MAPK, and Wnt/β-catenin signaling pathways. The PI3K/Akt signaling axis is also significantly enriched for transposon-induced mutations that predict pathway activation. This finding is consistent with the known relationship between activated RAS, Akt, and tumor maintenance (29, 30). In addition, GKC CCGs are enriched for genes involved in Ephrin receptor signaling,

Table 1. Signaling pathways enriched for CCGs

Signaling pathways and cellular processes	Percent tumor	Number CCG (GKC method)	*P* value	Number CCG (gCIS method)	*P* value	Representative genes	Analysis platform
Molecular mechanisms of cancer	100	13	2.25E-06	35	8.79E-07	*Crebbp*, *Gsk3b*, *Mll3*, *Pten*, and *Nsd1*	IPA
GO:0016568–chromatin modification	100	14	3.52E-05	34	3.26E-08	*Kdm6a*, *Mll3*, *Mll5*, *Myst3*, and *Nsd1*	DAVID
TGF-β	90	7	3.46E-06	16	1.5E-06	*Acvr2a*, *Crebbp*, *Smad2*, *Smad4*, and *Smurf2*	IPA
RAR activation	90	9	5.72E-06	21	1.27E-05	*Ncor1*, *Nsd1*, *Pdpk1*, and *Pik3r1*	IPA
HGF signaling	90	7	1.12E-05	21	7.69E-09	*Atf2*, *Dock1*, *Grb2*, *Ptk2*, *Ptpn11*, and *Rap1a*	IPA
ERK/MAPK	90	8	8.89E-05	19	2.84E-04	*Grb2*, *Mapk1*, *Pak1*, and *Ptk2*	IPA
Tight junction signaling	90	8	1.25E-03	17	9.91E-05	*Ash1l*, *Ctnna1*, *Inadl*, *Magi1*, and *Magi2*	KEGG
GO:0003682–chromatin binding	90	9	6.6E-03	22	3.04E-05	*Adnp*, *Arid4b*, *Gata6*, *Mbd1*, and *Ncoa1*	DAVID
PI3K/Akt	86	7	3.72E-05	15	2.14E-04	*Mapk1*, *Pdpki*, *Pik3ca*, *Pten*, and *Rps6kb1*	IPA
Integrin	86	8	1.48E-04	23	1.39E-05	*Arhgap5*, *Itgb1*, *Ptk2*, and *Rapgef1*	IPA
Ephrin receptor	86	7	3.7E-04	21	1.51E-05	*Abi1*, *Cdc42*, *Epha6*, *Gnaq*, and *Gna14*	IPA
Rac Signaling	86	5	1.25E-03	15	5.29E-05	*Cdc42*, *Iqgap1*, *Iqgap2*, *Map3k1*, and *Pak1*	IPA
Formation of filaments	81	10	6.75E-05	32	4.41E-05	*Akap13*, *Atxn2*, *Ctnnd1*, and *Fhit*	IPA
Wnt/β-catenin	76	5	1.02E-02	18	3.17E-04	*Csnk1d*, *Gnaq*, *Gsk3β*, *EP300*, and *Ppp2r5e*	IPA
Adherens junction	76	5	1.6E-02	15	7.42E-06	*Actn1*, *Cdh1*, *Crebbp*, *Ctnna1*, and *Ctnnd1*	KEGG

Analysis of CCGs using IPA, DAVID, and KEGG revealed several canonical signaling pathways and processes enriched for CCGs from *SB*-driven pancreatic tumors. Percent tumor is the proportion of tumors that had a mutation in at least one CCG found within the pathway; 48 GKC CCGs and 174 gCCGs were significantly enriched in canonical pathways identified by IPA. *P* values for pathway enrichment were adjusted for multiple testing using the Benjamini–Hochberg method for control of the false discovery rate.

Mann et al.

which is important for cytoskeletal reorganization and cell pro-liferation, human growth factor (HGF) signaling, which mediates cell growth through growth factor signaling, and retinoic acid receptor (RAR) signaling, which is involved in regulating cell growth and invasion.

We also used the Database for Annotation, Visualization and Integrated Discovery (DAVID) (31, 32) to identify cellular pro-cesses that are enriched in the pancreatic CCGs. DAVID is a functional annotation tool used to interrogate gene sets using over 40 annotation categories, including gene ontology terms, protein–protein interactions, and biological pathways. Chroma-tin modification was one of the most significantly enriched pro-cesses for CCGs (Table 1). Indeed, all tumors had a mutation in at least one gene encoding a histone-modifying enzyme. Several of these genes, including *Kdm6a* (33), *Mll3* (34), and *Mll5* (35), are mutated in several human cancers, pointing to a complex role for epigenetics in human cancer and in particular, pancreatic cancer. Filament assembly and specifically actin remodeling are also significantly enriched for GKC CCGs. Genes involved in adherens junctions and tight junctions identified using the Kyoto Encyclopedia of Genes and Genomes (KEGG) were also fre-quently mutated in *SB*-induced pancreatic cancers. These pro-cesses play important roles in cell invasion and metastasis.

Gene centric CISs and Their Potential Role in Pancreatic Cancer. The GKC method identifies CISs by looking for regions in the genome of a given kernel size in which *SB* insertions occur at a higher frequency than predicted by chance. We reasoned, however, that because the vast majority of CISs in pancreatic tumors encode TS genes and transposon insertions in TS genes are often randomly distributed across the coding region, the GKC method might miss a number of important CISs. We therefore decided to look for CISs by a second gene centric method that does not rely on pat-terns of clustered transposon insertions (36). This approach con-siders all uniquely mappable TA dinucleotides in the coding region of each RefSeq gene as a fraction of all uniquely mappable TA dinucleotides in the mouse genome. The population frequency of transposon insertions in each RefSeq is then calculated (after fil-tering insertions on transposon donor chromosomes). χ^2 analysis is used to calculate the probability of the transposon mutating a TA in a given gene with a higher frequency than predicted by chance.

Using this approach, we identified 671 gene centric CISs (gCISs; $P < 0.05$) that contained three or more intragenic inser-tions in at least three independent tumors (Dataset S4). Three tumors is the minimal number of tumors required to identify a CIS by the GKC method, and they represent 15% of our *SB* tu-mor cohort. The gCIS method identified 653 candidate cancer genes, 14 Riken clones, and 4 genomic markers; 92% of the GKC CISs were also identified by the gCIS computational method. We found significant enrichment of gene centric CCGs (gCCGs) among the genes listed in the Cancer Gene Census ($n = 34$, $P = 1.67E-12$) (Dataset S5). Importantly, we also found significant enrichment for gCCGs in the genes mutated in human pancre-atic cancer ($n = 53$, $P = 5.11E-09$) or located near sites of ge-nomic rearrangement in human pancreatic cancer ($n = 25$, $P = 1.80E-21$).

When we looked for canonical signaling pathways and pro-cesses using gCCGs, we found 402 additional genes involved in pathways and processes enriched for pancreatic CCGs that were identified by the GKC method. Rac signaling, involved in actin polymerization as well as HGF, ephrin receptor, integrin, and Wnt/β-catenin signaling pathways, showed significant enrichment for gCCGs (Table 1). In addition, genes involved in tight junc-tions and adherens junctions were significantly enriched for gCCGs as were genes involved in chromatin modification. These data indicate that the gCIS method identifies additional candi-date cancer genes important for pancreatic adenocarcinoma in our model.

CCGs in *SB*-Driven Pancreatic Cancer Predict Human Pancreatic Cancer Patient Survival. We next wanted to assess whether any of the GKC CCGs that we identified in our transposon screen had a significant impact on human pancreatic cancer. We used expression array data from human pancreatic tumors available from the National Center for Biotechnology Information Gene Expression Omnibus database (37, 38) (GSE21501) for which patient survival data were available (39). We considered a CCG as being validated if at least one of the probe sets on the array had a significant association with patient survival (based on Cox proportional hazards regression) after *P* value adjustment for multiple testing (*SI Materials and Methods*). Based on these criteria, 20 GKC CCGs were signifi-cantly associated with patient survival in this dataset. Fig. S2 shows the survival curves generated by dividing the samples into high and low expression groups at different percentiles; 14 of 20 genes showed a positive correlation between the predicted mutagenic effect of *SB* transposition in mouse pancreatic tumors (i.e., gene activation or inactivation) and gene expression levels associated with poor survival in the human tumors. The probability of ob-taining this result by chance was 0.03. This work reports *CRKRS*, *PARD6G*, *PUM2*, *SOCS5*, and *ZFX* as candidate oncogenes and *AKAP13*, *CTNND1*, *DYRK1A*, *FBXO11*, *GSK3B*, *MYO1D*, *VGLL4*, *ZC3H7A*, and *ZFAND3* as candidate tumor suppressors in human pancreatic cancer.

We then interrogated a tissue microarray comprised of three-replicate 1-mM cores from 150 patients with pancreatic adeno-carcinoma (40) for levels of protein encoded by frequently mu-tated CCGs found in enriched signaling pathways. For two proteins, CTNND1 and GNAQ, we observed a decrease or ab-sence of staining in tumors with intact staining in adjacent benign ducts or acini present within the same core (Fig. 4). CTNND1 is membrane-bound and plays a role in adherens junctions by regulating E-cadherin (41); it has also been shown to regulate WNT signaling (42). GNAQ is a cytoplasmic guaninine–nucle-otide binding protein that signals to RhoA and is implicated in cell proliferation and migration (43). Low staining for CTNND1 ($P = 0.023$) was significantly associated with poor survival (Fig. 4) using a univariate Cox analysis of overall survival (*SI Materials and Methods*), whereas low staining for GNAQ showed a bor-derline significant association with poor survival ($P = 0.051$). Analysis of CTNND1 staining in a second independent pancre-atic cancer tissue microarray of 142 patient samples (44, 45) confirmed that decreased CTNND1 is significantly associated with poor survival in pancreatic cancer patients who underwent operative resection (Fig. S3). These data also substantiate that disruption of genes participating in cell–cell interactions and regulation of cell migration in *SB*-driven pancreatic tumors have biological relevance to disease.

Exome Sequencing from Human Pancreatic Cancer Patients Uncovers Damaging Point Mutations. Finally, we investigated the coding mutation status of the 136 GKC CCGs in human pancreatic cancer patient samples. We queried the Australian Pancreatic Cancer Genome Initiative exome sequence mutation discovery database, which was created from a collection of 60 pancreatic cancer patient DNAs with matched normal controls. Surprisingly, 68 GKC CISs exhibited coding mutations in at least one patient. We validated nonsilent coding mutations in nine human homologs of the mouse GKC CISs in these samples using targeted PCR and Ion Torrent sequencing at >1,000-fold depth of coverage. These homologs are *ACVR2A*, *AFF4*, *AP1G1*, *CREBBP*, *MEIS2*, *MKLN1*, *MLL3*, *SMAD4*, and *THSD7A* (Dataset S6). In addition, mutations in *CTNNA3* and *MAP2K4*, two human homologs of *SB* CCGs iden-tified using the gCIS method, were also validated. Loss of *SMAD4* is a well-documented driver in human pancreatic cancer and mouse models. The work by Jones et al. (5) previously identified mutations in *MLL3*, a member of the mixed lineage leukemia gene family, in both their exome discovery and validation screens for
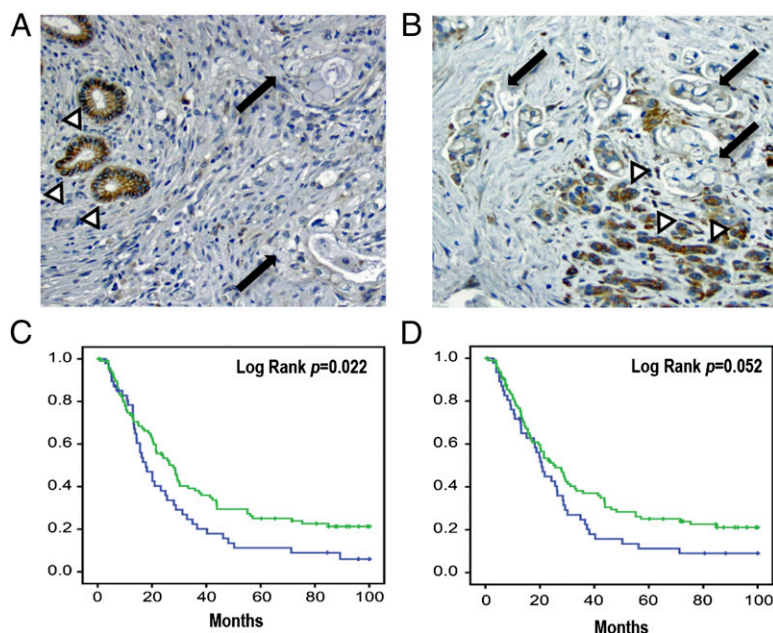
Fig. 4. CTNND1 and GNAQ show absent or weak staining in human pancreatic tumors. Immunohistochemistry was performed on a human pancreatic tissue microarray for (A) CTNND1 and (B) GNAQ. Arrows indicate tumors with weak or absent staining, whereas adjacent benign ducts or acini (indicated by white arrowheads) verify the presence of intact staining in tissue sections. Weak or absent staining of (C) CTNND1 (log rank *P* = 0.022) and (D) GNAQ (log rank *P* = 0.051) is predictive of poor survival. Kaplan–Meier plots (C and D) of patient survival represent two patient groups dichotomized into the top two tertiles (green) vs. bottom tertile (blue) using the histoscore for high and low staining.

pancreatic cancer mutations. *CREBBP*, which encodes an acetylase that targets histones and nonhistones, and *CTNNA3*, an ortholog of *CTNND1* also involved in cell adhesion, were also identified in their discovery screen.

Seven of the validated GKC CISs are unique. The majority of the mutations in these genes are missense, although nonsense mutations were identified in two genes—*ACVR2A*, which encodes a type II receptor of the TGF-β superfamily that also participates in integrin signaling, and *MAP2K4*, which is involved in JUN kinase activation. Interestingly, all genes with validated mutations are predicted to be potential tumor suppressors by our screen. We also validated mutations in orthologs of four GKC CISs that encode proteins with similar biological function. *AFF2* is an ortholog of the GKC CIS *AFF4*, which encodes proteins involved in both splicing and transcriptional control. *DOCK2* and *DOCK3* are orthologs of the GKC CIS *DOCK1* (*DOCK180*), which is involved in Rac signaling. *THSD7B*, mutated in the discovery screen by Jones et al. (5) and an ortholog of *THSD7A*, is also mutated in the Australian Pancreatic Cancer Genome Initiative cohort. Given the heterogeneity of mutations in pancreatic cancer, it is encouraging that many of our *SB* CCGs have validated mutations in a cohort of only 60 patients. Additional experimentation is required to determine the impact of these mutations on disease development and prognosis.

Discussion

We report an *SB* insertional mutagenesis screen to identify loci that cooperate with oncogenic *Kras* to drive pancreatic adenocarcinoma in the mouse. *SB*-driven pancreatic adenocarcinomas show all stages of mPanIN that develop into early noninvasive adenocarcinoma and finally, invasive, highly metastatic adenocarcinoma. Importantly, these tumors also have a high desmoplastic component, a predominant histopathic feature of human pancreatic cancer. The T2Onc3 transposon proved to be more potent than T2Onc2 in inducing metastatic tumors. The exact mechanism for the difference between the two transposons in driving pancreatic cancer is unknown. One possibility is that the location of the transposon

concatemer donor influences the development of the tumor. The T2Onc3 donor resides on chromosome 9, and pancreatic cancer genes in close proximity may be frequently mutated in these tumors because of local hopping.

Both T2Onc2 and T2Onc3 cohorts exhibited considerably higher numbers of nonredundant insertions per tumor relative to the number of transposons in the donor concatemer (fivefold greater insertions for T2Onc2 and 20-fold greater insertions for T2Onc3 on average). The large number of mapped insertions (19,927 from 21 independent tumors) is likely because of the fact that many insertions are background passengers as opposed to driver mutations, and it also reflects the oligoclonality of these tumors. Using both the GKC and the gCIS methods, we identified 681 statistically significant CISs that comprise 543 pancreatic CCGs. The tumor heterogeneity makes it difficult to identify co-occurrence of insertions in individual subclones. One way to begin to address this issue is to use laser capture microdissection to determine the transposon insertion profiles in tumor subclones. Ultimately, it will take single-cell sequencing to understand the degree of heterogeneity in pancreatic and other solid tumors.

The majority of the genes that we identified in our *SB* pancreatic insertional mutagenesis screen (90%) are predicted to be disrupted based on the orientation of the transposon with respect to the gene. For most CISs, only one transposon insertion is observed per tumor, although there are examples of tumors with multiple insertions that contribute to a CIS. We believe that these singly mutated genes do play a role in pancreatic cancer for several reasons. Many of these TS genes function in known signaling pathways in cancer, and they are found mutated in human cancer with a frequency greater than predicted by chance. Indeed, 75 CCGs overlap with genes mutated or deleted in human pancreatic adenocarcinoma from published sequencing efforts. In addition, although solid tumors induced by *SB* seem to select for loss of function mutations (13, 45), *SB*-induced hematopoietic cancers seem to select for oncogenes. This finding argues that there is something special about solid tumors that selects for loss of function mutations. Some of the CISs that we identified may represent haploinsufficient

tumor suppressors, a recent example being *Fbxo11* in B-cell lymphoma (46). Alternatively, acquired point mutation, rearrangement, or epigenetic silencing may be the preferred mechanism for inactivating the second allele in solid tumors.

Analysis of the human pancreatic cancer genome by sequencing SNP and Comparative Genomic Hybridization (CGH) arrays has shown that chromosome loss or gene deletions are frequent events in human pancreatic cancer (5, 6, 47). Missense mutations predominate the pancreatic genome mutational landscape. Using an algorithm to predict the significance of cancer-associated mutations (i.e., not passengers), the work by Jones et al. (5) reported that 17% of the missense mutations identified in their discovery set for human pancreatic cancer are likely to contribute to tumorigenesis. Our *SB*-driven pancreatic tumors provide an enriched dataset of frequently mutated genes that include many of the genes mutated in the human discovery set. These genes include *Mecom* (mutated in 57% of *SB*-driven pancreatic tumors), *Mll5*, *Ptprk*, *Zc3h7a* (each mutated in 43% of tumors), and *Ino80* (mutated in 38% of tumors). We also find transposon insertions in several genes identified in the work by Campbell et al. (6) to be either deleted (*PKT2*, *SLC12A8*, and *XPO7*) or involved in intra- (*KDM2A* and *MYO1D*) or interchromosomal (*MLLT10*) rearrangements that are each mutated in >25% of the *SB* pancreatic tumors. The high mutation frequency of these genes and others in our *SB* screen provides evidence that many of the CCGs may indeed be drivers of pancreatic cancer. We also identified nonsilent mutations in eleven CCGs in human pancreatic cancer patient samples from the Australian Pancreatic Cancer Genome Initiative. We anticipate that additional mutations in human homologs of *SB* CCGs will be identified in human pancreatic cancer as more patient samples are sequenced.

The most significantly mutated gene identified by both the GKC and gCIS methods is *Pten*. Mutations in this tumor suppressor gene have not been identified in pancreatic cancer, although the chromosomal region in which it lies on 10q23 does undergo loss of heterozygosity (48–50). Inactivation of *Pten* in the mouse, recently shown to cooperate with oncogenic *Kras* to drive pancreatic adenocarcinoma (51), may be the easiest way to deregulate Akt signaling in the mouse. Although *TP53* mutations are frequent in human pancreatic cancer, we do not detect *Trp53* as a CIS in our screen. However, we do find mutations in a number of genes in the *Trp53* pathway, including *Crebbp*, *Jmy*, and *Mapk8*. *Usp9x*, the second most significantly mutated gene in our screen and predicted to be inactivated, has not been associated as a tumor suppressor with any cancer, although point mutations have been identified in breast (52), lung (53), and ovarian cancers (26). *USP9x* encodes a deubiquitinase that has been shown to stabilize MCL1 in several tumor types (54). We identify several genes in our screen involved in ubiquitin-mediated protein degradation, a few of which (*ARIH1*, *FBXO11*, *UBR5*, and *USP24*) have mutations in human cancer. Fbxo11 has been shown to modulate TGF-β signaling in a mouse mutant (55) and influence Trp53 neddylation (56). Ubr5, also known as EDD, has a number of potential targets, including β-catenin (57).

Remarkably, 10% of the pancreatic CCGs that we identify function in chromatin remodeling, and 100% of tumors had a mutation in at least one of these genes. *Mll3* is a component of the Asc-2 containing (Ascom) complex involved in H3K4 trimethylation, a histone modification associated with gene activation (58). This complex also contains Kdm6a, suggesting that this H3K27 trimethyl-demethylase may also have a role in methylating H3K4. Mutations were also found in *Whsc1l1* (*Nsd3*), a methyltransferase known to target both H3K4 and H3K27. Analyses of methylation patterns and patient outcome in human pancreatic ductal adeno-

carcinoma have shown that low levels of histone methylation are generally predictors of poor survival (40, 59). Recent findings from exome sequencing of pancreatic neuroendocrine tumors show that chromatin remodeling and specifically, inactivating mutations in *MEN1*, a component of MLL1- and MLL2-H3K4 methyltransferase complexes, play important roles in this disease as well (60). Identification of the genes regulated by these epigenetic marks will be critical to understanding how epigenetic mechanisms can modulate pancreatic cancer.

Our data support the observations made in the work by Jones et al. (5) that a limited number of canonical signaling pathways are mutated in the majority of pancreatic tumors. We find significant enrichment for *SB* CCGs in known signaling pathways involved in pancreatic cancer, including TGF-β, Wnt/β-catenin, and integrin signaling. Importantly, we identify genes involved in these enriched pathways that have not been reported as mutated in human pancreatic cancer. The mutational heterogeneity in *SB* tumors may arise from the plasticity of pathways that permits deregulation by a number of distinct genetic alterations. This finding argues for a need to better understand pathway perturbations in cancer at the cellular level rather than at the gene level.

SB insertional mutagenesis shows great power for identifying candidate cancer genes with direct relevance to human cancers. Our model of *SB*-driven pancreatic adenocarcinoma shows all stages of pancreatic lesions leading up to adenocarcinoma and metastasis. The ease of mapping transposon insertion sites within the cancer genome makes it possible to interrogate the gene perturbations that occur at each stage, which can potentially lead to the identification of cancer drivers required for the initiation, progression, and metastasis of pancreatic adenocarcinoma. The significant overlap of our findings with sequencing data from human tumors highlights the relevance of this pancreatic cancer mouse model to human pancreatic adenocarcinoma. Data from the *SB*-driven pancreatic tumors will undoubtedly aid in the prioritization and validation of forthcoming human sequencing data from pancreatic adenocarcinoma.

Materials and Methods

Mice. We used the following alleles to generate a mouse model of pancreatic cancer: *LSL-Kras*^G12D (14), *Pdx1*-Cre (15), T2Onc2 (6113) (23), T2Onc3 (12740), and *Rosa26-LSL-SB11* (61). The resulting cohorts were on a mixed B6.129 genetic background. All animals were monitored on a biweekly basis in accordance with the Institutional Animal Care and Use Committee guidelines. Gross necropsies were performed, and one-half of the pancreas was snap-frozen; the other one-half (retaining the duodenum) was fixed and paraffin-embedded. All masses larger than 5 mm were recovered; one-half was snap-frozen, and the other one-half was fixed and paraffin-embedded.

Cloning and Mapping Transposon Insertions Sites. Isolation of the transposon insertion sites was performed using splinkerette PCR to produce barcoded PCR products that were pooled and sequenced on the 454 GS-Titanium sequencers (Roche) platform. Reads from sequenced tumors were mapped to the mouse genome assembly National Center for Biotechnology Information m37 and merged together to identify nonredundant *SB* insertion sites (*SI Materials and Methods*).

1. Jemal A, Siegel R, Xu J, Ward E (2010) Cancer statistics, 2010. *CA Cancer J Clin* 60: 277–300.
2. Stathis A, Moore MJ (2010) Advanced pancreatic carcinoma: Current treatment and future challenges. *Nat Rev Clin Oncol* 7:163–172.
3. Maitra A, Fukushima N, Takaori K, Hruban RH (2005) Precursors to invasive pancreatic cancer. *Adv Anat Pathol* 12:81–91.
4. Hansel DE, Kern SE, Hruban RH (2003) Molecular pathogenesis of pancreatic cancer. *Annu Rev Genomics Hum Genet* 4:237–256.
5. Jones S, et al. (2008) Core signaling pathways in human pancreatic cancers revealed by global genomic analyses. *Science* 321:1801–1806.
6. Campbell PJ, et al. (2010) The patterns and dynamics of genomic instability in metastatic pancreatic cancer. *Nature* 467:1109–1113.
7. Aguirre AJ, et al. (2003) Activated Kras and Ink4a/Arf deficiency cooperate to produce metastatic pancreatic ductal adenocarcinoma. *Genes Dev* 17:3112–3126.
8. Hingorani SR, et al. (2003) Preinvasive and invasive ductal pancreatic cancer and its early detection in the mouse. *Cancer Cell* 4:437–450.
9. Bardeesy N, et al. (2006) Both p16(Ink4a) and the p19(Arf)-p53 pathway constrain progression of pancreatic adenocarcinoma in the mouse. *Proc Natl Acad Sci USA* 103: 5947–5952.
10. Bardeesy N, et al. (2006) Smad4 is dispensable for normal pancreas development yet critical in progression and tumor biology of pancreas cancer. *Genes Dev* 20: 3130–3146.
11. Hingorani SR, et al. (2005) Trp53R172H and KrasG12D cooperate to promote chromosomal instability and widely metastatic pancreatic ductal adenocarcinoma in mice. *Cancer Cell* 7:469–483.
12. Hruban RH, et al. (2006) Pathology of genetically engineered mouse models of pancreatic exocrine cancer: Consensus report and recommendations. *Cancer Res* 66: 95–106.
13. Copeland NG, Jenkins NA (2010) Harnessing transposons for cancer gene discovery. *Nat Rev Cancer* 10:696–706.
14. Jackson EL, et al. (2001) Analysis of lung tumor initiation and progression using conditional expression of oncogenic K-ras. *Genes Dev* 15:3243–3248.
15. Gu G, Dubauskaite J, Melton DA (2002) Direct evidence for the pancreatic lineage: NGN3+ cells are islet progenitors and are distinct from duct progenitors. *Development* 129:2447–2457.
16. Gold DV, Karanjawala Z, Modrak DE, Goldenberg DM, Hruban RH (2007) PAM4-reactive MUC1 is a biomarker for early pancreatic adenocarcinoma. *Clin Cancer Res* 13: 7380–7387.
17. Fujita H, et al. (2010) alpha-Smooth muscle actin expressing stroma promotes an aggressive tumor biology in pancreatic ductal adenocarcinoma. *Pancreas* 39:1254–1262.
18. de Ridder J, Uren A, Kool J, Reinders M, Wessels L (2006) Detecting statistically significant common insertion sites in retroviral insertional mutagenesis screens. *PLoS Comput Biol* 2:e166.
19. Krzywinski M, et al. (2009) Circos: An information aesthetic for comparative genomics. *Genome Res* 19:1639–1645.
20. Starr TK, et al. (2009) A transposon-based genetic screen in mice identifies genes altered in colorectal cancer. *Science* 323:1747–1750.
21. Starr TK, et al. (2011) A Sleeping Beauty transposon-mediated screen identifies murine susceptibility genes for adenomatous polyposis coli (Apc)-dependent intestinal tumorigenesis. *Proc Natl Acad Sci USA* 108:5765–5770.
22. March HN, et al. (2011) Insertional mutagenesis identifies multiple networks of cooperating genes driving intestinal tumorigenesis. *Nat Genet* 43:1202–1209.
23. Dupuy AJ, Akagi K, Largaespada DA, Copeland NG, Jenkins NA (2005) Mammalian mutagenesis using a highly mobile somatic Sleeping Beauty transposon system. *Nature* 436:221–226.
24. Futreal PA, et al. (2004) A census of human cancer genes. *Nat Rev Cancer* 4:177–183.
25. Wood LD, et al. (2007) The genomic landscapes of human breast and colorectal cancers. *Science* 318:1108–1113.
26. Network TCGAR; Cancer Genome Atlas Research Network (2011) Integrated genomic analyses of ovarian carcinoma. *Nature* 474:609–615.
27. IPA *Ingenuity Systems*. Available at http://www.ingenuity.com. Accessed August 17, 2011.
28. Sjöblom T, et al. (2006) The consensus coding sequences of human breast and colorectal cancers. *Science* 314:268–274.
29. Lim KH, Counter CM (2005) Reduction in the requirement of oncogenic Ras signaling to activation of PI3K/AKT pathway during tumor maintenance. *Cancer Cell* 8:381–392.
30. Singh A, et al. (2009) A gene expression signature associated with "K-Ras addiction" reveals regulators of EMT and tumor cell survival. *Cancer Cell* 15:489–500.
31. Huang W, Sherman BT, Lempicki RA (2009) Systematic and integrative analysis of large gene lists using DAVID bioinformatics resources. *Nat Protoc* 4:44–57.
32. Huang W, Sherman BT, Lempicki RA (2009) Bioinformatics enrichment tools: Paths toward the comprehensive functional analysis of large gene lists. *Nucleic Acids Res* 37: 1–13.
33. van Haaften G, et al. (2009) Somatic mutations of the histone H3K27 demethylase gene UTX in human cancer. *Nat Genet* 41:521–523.
34. Balakrishnan A, et al. (2007) Novel somatic and germline mutations in cancer candidate genes in glioblastoma, melanoma, and pancreatic carcinoma. *Cancer Res* 67: 3545–3550.
35. Damm F, et al. (2011) Prognostic importance of histone methyltransferase MLL5 expression in acute myeloid leukemia. *J Clin Oncol* 29:682–689.
36. Brett BT, et al. (2011) Novel molecular and computational methods improve the accuracy of insertion site analysis in Sleeping Beauty-induced tumors. *PLoS One* 6: e24668.
37. Edgar R, Domrachev M, Lash AE (2002) Gene Expression Omnibus: NCBI gene expression and hybridization array data repository. *Nucleic Acids Res* 30:207–210.
38. Barrett T, et al. (2011) NCBI GEO: Archive for functional genomics data sets—10 years on. *Nucleic Acids Res* 39:D1005–D1010.
39. Stratford JK, et al. (2010) A six-gene signature predicts survival of patients with localized pancreatic ductal adenocarcinoma. *PLoS Med* 7:e1000307.
40. Manuyakorn A, et al. (2010) Cellular histone modification patterns predict prognosis and treatment response in resectable pancreatic adenocarcinoma: Results from RTOG 9704. *J Clin Oncol* 28:1358–1365.
41. Ishiyama N, et al. (2010) Dynamic and static interactions between p120 catenin and E-cadherin regulate the stability of cell-cell adhesion. *Cell* 141:117–128.
42. Casagolda D, et al. (2010) A p120-catenin-CK1epsilon complex regulates Wnt signaling. *J Cell Sci* 123:2621–2631.
43. Lutz S, et al. (2007) Structure of Galphaq-p63RhoGEF-RhoA complex reveals a pathway for the activation of RhoA by GPCRs. *Science* 318:1923–1927.
44. Chang DK, et al. (2009) Margin clearance and outcome in resected pancreatic cancer. *J Clin Oncol* 27:2855–2862.
45. Biankin AV, et al. (2009) Expression of S100A2 calcium-binding protein predicts response to pancreatectomy for pancreatic cancer. *Gastroenterology* 137:558–568.
46. Duan S, et al. (2012) FBXO11 targets BCL6 for degradation and is inactivated in diffuse large B-cell lymphomas. *Nature* 481:90–93.
47. Harada T, et al. (2008) Genome-wide DNA copy number analysis in pancreatic cancer using high-density single nucleotide polymorphism arrays. *Oncogene* 27:1951–1960.
48. Birnbaum DJ, et al. (2011) Genome profiling of pancreatic adenocarcinoma. *Genes Chromosomes Cancer* 50:456–465.
49. Okami K, et al. (1998) Analysis of PTEN/MMAC1 alterations in aerodigestive tract tumors. *Cancer Res* 58:509–511.
50. Sakurada A, et al. (1997) Infrequent genetic alterations of the PTEN/MMAC1 gene in Japanese patients with primary cancers of the breast, lung, pancreas, kidney, and ovary. *Jpn J Cancer Res* 88:1025–1028.
51. Hill R, et al. (2010) PTEN loss accelerates KrasG12D-induced pancreatic cancer development. *Cancer Res* 70:7114–7124.
52. Kan Z, et al. (2010) Diverse somatic mutation patterns and pathway alterations in human cancers. *Nature* 466:869–873.
53. Ding L, et al. (2008) Somatic mutations affect key pathways in lung adenocarcinoma. *Nature* 455:1069–1075.
54. Schwickart M, et al. (2010) Deubiquitinase USP9X stabilizes MCL1 and promotes tumour cell survival. *Nature* 463:103–107.
55. Tateossian H, et al. (2009) Regulation of TGF-beta signalling by Fbxo11, the gene mutated in the Jeff otitis media mouse mutant. *Pathogenetics* 2:5.
56. Abida WM, Nikolaev A, Zhao W, Zhang W, Gu W (2007) FBXO11 promotes the Neddylation of p53 and inhibits its transcriptional activity. *J Biol Chem* 282: 1797–1804.
57. Hay-Koren A, Caspi M, Zilberberg A, Rosin-Arbesfeld R (2011) The EDD E3 ubiquitin ligase ubiquitinates and up-regulates beta-catenin. *Mol Biol Cell* 22:399–411.
58. Lee S, et al. (2006) Coactivator as a target gene specificity determinant for histone H3 lysine 4 methyltransferases. *Proc Natl Acad Sci USA* 103:15392–15397.
59. Wei Y, et al. (2008) Loss of trimethylation at lysine 27 of histone H3 is a predictor of poor outcome in breast, ovarian, and pancreatic cancers. *Mol Carcinog* 47:701–706.
60. Jiao Y, et al. (2011) DAXX/ATRX, MEN1, and mTOR pathway genes are frequently altered in pancreatic neuroendocrine tumors. *Science* 331:1199–1203.
61. Dupuy AJ, et al. (2009) A modified sleeping beauty transposon system that can be used to model a wide variety of human cancers in mice. *Cancer Res* 69:8150–8156.

Mann et al.